0026-895X/03/6402-269–278$7.00
MOLECULAR PHARMACOLOGY
Copyright © 2003 The American Society for Pharmacology and Experimental Therapeutics
Mol Pharmacol 64:269–278, 2003

Vol. 64, No. 2
2551/1077767
Printed in U.S.A.

The Mechanism of Action of Aniracetam at Synaptic α-Amino-3-hydroxy-5-methyl-4-isoxazolepropionic Acid (AMPA) Receptors: Indirect and Direct Effects on Desensitization

J. JOSH LAWRENCE,[1] STEPHAN BRENOWITZ,[2] and LAURENCE O. TRUSSELL

Oregon Hearing Research Center and Vollum Institute, Oregon Health and Science University, Portland, Oregon

Received March 24, 2003; accepted April 16, 2003

This article is available online at http://molpharm.aspetjournals.org

ABSTRACT

The mechanism of action of aniracetam on α-amino-3-hydroxy-5-methyl-4-isoxazolepropionic acid (AMPA) receptors was examined in outside-out patches and at glutamatergic synapses in neurons of the chick cochlear nucleus. A combination of rapid-flow analysis, using glutamate as an agonist, and kinetic modeling indicated that aniracetam slows both the rate of channel closing, and the microscopic rates of desensitization, even for partially liganded receptors. Little effect was observed on the rate of recovery from desensitization or on the response to the weakly desensitizing agonist kainate. Aniracetam's effects on receptor deactivation saturated at lower concentrations than its effects on desensitization, suggesting that cooperativity between homologous binding sites was required to regulate desensitization. Analysis of responses to paired pulses of agonist also indicated that AMPA receptors must desensitize partially even after agonist exposures too brief to permit rebinding. In the presence of aniracetam, evoked excitatory synaptic currents (EPSCs) and miniature EPSCs in low quantal-content conditions had decay times similar to the time course of receptor deactivation. Under these conditions, the time course of both transmitter release and clearance must be <1 to 2 ms. However, in high quantal-content conditions, the evoked EPSC in aniracetam decayed with a time course intermediate between deactivation and desensitization, suggesting that the time course of transmitter clearance is prolonged because of pooling of transmitter in the synaptic cleft. Moreover, by comparing the amounts of paired-pulse synaptic depression and patch desensitization prevented by aniracetam, we conclude that significant desensitization occurs in response to rebinding of transmitter to the AMPA receptors.

The nootropic benzoylpiperidine aniracetam has been used extensively in studies characterizing the function of α-amino-3-hydroxy-5-methyl-4-isoxazolepropionate (AMPA) receptors throughout the brain (e.g., Isaacson and Nicoll, 1991; Tang et al., 1991; Vyklicky et al., 1991). Studies using rapid flow analysis in neurons (Vyklicky et al., 1991) or expressed glutamate receptor 1 (Partin et al., 1996) suggested that the primary action of the compound is to slow the rate of channel closure. Such an effect could account both for the slowing of receptor deactivation and for slowed desensitization, because by buffering channels in an open configuration, the drug will delay their accumulation in a desensitized state. Here, drugs may alter macroscopic desensitization indirectly without interacting specifically with structural elements involved in the desensitization itself. An alternative hypothesis is that aniracetam promotes reopening by slowing both desensitization and unbinding, without effects on channel closure per se (Arai et al., 1996). This is suggested by cases in which drugs potentiate glutamate responses and remove desensitization, with minimal effect on deactivation (Arai et al., 1996, 2000). However, neither of these interpretations accounts for a major feature of aniracetam: it blocks paired pulse depression of synaptic transmission. Finally, interpretation of aniracetam's effects must account for that fact that functional AMPA receptors may be composed of two dimers (Sun et al., 2002). Thus, one would expect multiple binding sites for allosteric modulators such as aniracetam, and the effects of the drug might depend on the degree of ligation. It is important, therefore, to develop a conceptual framework that can account both for the normal behavior of the receptor and for the targeting of drug action to distinct functions of the receptor.

This work was supported by National Institutes of Health grants DC02004 and NS28901.

[1] Present address: Unit on Cellular and Synaptic Physiology, Laboratory of Cellular and Synaptic Neurophysiology, National Institute of Child Health and Human Development, National Institutes of Health, Bethesda, Maryland.
[2] Present address: Department of Neurobiology, Harvard Medical School, 220 Longwood Ave, Boston, Massachusetts 02115.

ABBREVIATIONS: AMPA, α-amino-3-hydroxy-5-methyl-4-isoxazolepropionate; EPSC, excitatory postsynaptic current; BAPTA, 1,2-bis(2-aminophenoxy)ethane-*N*,*N*,*N*′,*N*′-tetraacetic acid; SR-95531, 2-(3-carboxyl)-3-amino-6-(4-methoxyphenyl)-pyridazinium bromide; DMSO, dimethyl sulfoxide; P_o, open probability; GYKI 52466, 1-(4-aminophenyl)-methoxy-7,8-methylenedioxy-5H-2,3- benzodiazepine hydrochloride; mEPSC, miniature excitatory postsynaptic current; eEPSC, evoked excitatory postsynaptic current; PPD, paired-pulse depression.

In this study, we explored the effects of aniracetam on AMPA receptors in neurons of the chick cochlear nucleus magnocellularis. Somatic excitatory synapses cover nearly 50% of the somatic surface area in nucleus magnocellularis (Parks, 1981). The accessibility of these receptors to patch-clamp analysis presents an unusual opportunity for a kinetic analysis of synaptic receptors to accompany analysis of synaptic transmission. We find that aniracetam slows receptor deactivation, desensitization, and synaptic currents and reduces paired-pulse depression of the EPSC. Furthermore, aniracetam may interact with distinct functional processes of the receptor in a concentration-dependent manner. Finally, our data confirm that receptor desensitization is strongly dependent on the quantal content of release, as at high release levels glutamate clearance is markedly delayed.

Materials and Methods

Excised Patch Recordings. Neurons of the avian nucleus magnocellularis were enzymatically dissociated from tissue chunks microdissected from brain slices as described previously (Raman and Trussell, 1992). The neurons were plated onto poly-D-lysine–coated glass coverslips and allowed to adhere for 20 min. Isolated neurons were visualized with a Nikon inverted microscope using phase contrast at 40×. Intracellular solution contained 70 mM Cs_2SO_4, 85 mM sucrose, 4 mM NaCl, 1 mM $MgCl_2$, 10 mM HEPES, and 5 mM BAPTA, buffered to pH 7.3 with CsOH and osmolarity adjusted to 285 to 295 mOsM. For rapid application of 10 mM glutamate to patches, a θ-shaped pipette attached to a piezoelectric translator was used as described previously (Raman et al., 1994) except that solution delivery through the θ-shaped pipette was driven by nitrogen pressure. Control solutions contained normal Ringer's solution with 200 μM DL-aminophosphonovaleric acid and 10 μM 7-chlorokynurenic acid. Agonist solutions contained the above plus 10 mM glutamate. The agonist-containing solution was diluted by 5% with H_2O. The patch was blown out after the recording and the solution exchange time was then measured using the junction potential. The 10 to 90% solution exchange time was <250 μs. In some experiments, the contents of the θ-shaped pipette were changed to normal Ringer's solution and Ringer's solution diluted with H_2O to 10% yielding larger junction potentials and a more accurate measurement of solution exchange time. The contents of the θ-shaped pipette were switched manually with the use of stopcocks and occurred with a time constant of about 5 s. Data were Bessel filtered at 10 kHz and digitized at 20 to 40 kHz with pClamp6 software (Axon Instruments). We have previously shown that the kinetics of AMPA receptors in acutely dissociated preparations are unaffected by enzymatic treatment and are kinetically indistinguishable from those in brain slices (Lawrence and Trussell, 2000).

Curve Fitting and Simulations. Analysis and curve-fitting was performed with Origin (OriginLab Corp, Northampton, MA), Clampfit (Axon Instruments, Union City, CA), and Igor (Wavemetrics, Lake Oswego, OR). Data are compared with the results of a kinetic model shown below. A more complex exponential fit was accepted only if at least a 2-fold improvement in the χ^2 value was observed. Unless stated otherwise, results are presented as mean ± S.E.

Simulations were performed with SCoP software (Simulation Resources). The kinetic model shown in Scheme 1 was employed to interpret the results. Rates are listed in Table 1. In simulations, K_f, K_b', and K_b'' were doubled to account for higher probability of association and dissociation of two binding sites. This cyclic model, the conceptual foundation for more complex AMPA/kainate receptor gating schemes (Raman and Trussell, 1992, 1995b; Partin et al., 1996; Hausser and Roth, 1997; Heckmann and Dudel, 1997), accounts for several key features of the receptor, including multiple ligand binding sites and desensitization from partially liganded closed states (the C1-D1 transition). In the range of glutamate concentrations likely to occur during synaptic transmission, this minimal model reproduces most major kinetic features of the AMPA receptor that have been observed experimentally, such as rates of desensitization and deactivation, paired-pulse desensitization, and resensitization.

Slice Recordings. Brainstem slices (250–300 μm) were prepared from embryonic day 18 chick embryos in an oxygenated saline containing 140 mM NaCl, 20 mM glucose, 10 mM HEPES, 5 mM KCl, 3 mM $CaCl_2$, and 1 mM $MgCl_2$, pH 7.35. During recordings, slices were perfused with room temperature saline at 2 to 4 ml/min in a 1-ml chamber. Neurons were viewed with a Zeiss Axioskop and Olympus 60× water immersion lens using Nomarski optics and infrared illumination. For measurement of EPSCs, saline was supplemented with 100 μM DL-aminophosphonovaleric acid, 10 μM 7-Cl-kynurenate, 10 μM SR-95531, and 2 μM strychnine. Neurons in brain slices were voltage-clamped with an Axopatch 200B amplifier (Axon Instruments). Electrode series resistances (2–8 MΩ) were compensated 80 to 95%. Pipettes were filled with an intracellular solution containing 125 mM Cs-methanesulfonate, 15 mM CsCl, 10 mM HEPES, 5 mM BAPTA, and 1 mM $MgCl_2$, pH 7.25. Spontaneous mEPSCs were obtained at a holding potential of −60 mV. Currents were filtered at 10 kHz and sampled at 50 kHz. Events were detected using a template detection algorithm implemented in Axograph software (Axon Instruments). Evoked synaptic responses in neurons clamped to −30 mV were obtained by positioning a stimulus electrode (1.5–3 MΩ) onto nearby myelinated fibers, and individual auditory nerve axons stimulated by 100 to 200 μs, 5 to 50 V pulses delivered by an isolated stimulus unit (AMPI Iso-flex). Currents were filtered at 5 to 10 kHz and sampled at 20 to 50 kHz. Aniracetam stocks (0.5 M, 100×) were prepared in DMSO and added to extracellular solutions immediately before use. The final working concentration of aniracetam was 5 mM, and aniracetam-containing solutions included 1% (v/v) DMSO. For all experiments using aniracetam, control extracellular solutions were also supplemented with 1% DMSO. Chemicals and drugs were obtained from Sigma (St.

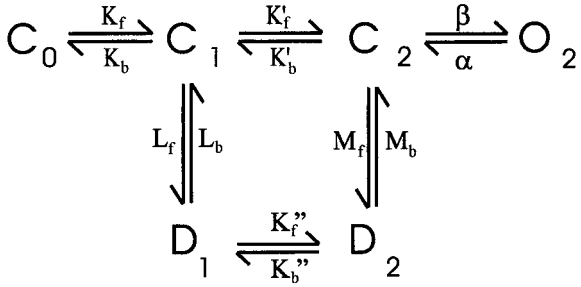

Scheme 1. C, closed states; O, open states; D, desensitized states. Numbers indicate number of agonist molecules bound.

TABLE 1

Rate constants used in quantitative model of aniracetam action

Numbers in bold are rates that were substantially altered to account for the action of 5 mM aniracetam. Other rates were altered by 33% or less.

Rate	Control	Aniracetam
	s^{-1}	
K_f	10^{7a}	10^{7a}
K_b	300	300
K_b'	30,000	30,000
K_b''	86[b]	80[b]
L_f	900	**200**
L_b	500	375
M_f	5,000	**1,200**
M_b	8	6
α	2875	**800**
β	20,000	20,000

[a] Units are $M^{-1} \cdot s^{-1}$.
[b] Rate changed to account for microscopic reversibility.

Louis, MO), RBI/Sigma (Natick, MA), and Tocris Cookson (Ballwin, MO).

Results

Effects of Aniracetam on Desensitization and Deactivation. Pulses of 10 mM glutamate, lasting 100 ms, were applied to excised patches in the presence of 0 to 5 mM aniracetam (Fig. 1; Table 2). In the absence of aniracetam, such applications induced currents that desensitized in two exponential phases, having a dominant component of 1.1 ± 0.05 ms and a minor component of 4.0 ± 0.3 ms (n = 6), in accordance with previous observations (Raman and Trussell, 1992; Lawrence and Trussell, 2000). Figure 1A illustrates a control response and exponential fits to the onset of desensitization. The inset displays the residuals of the single and double exponential fits, showing that the latter provided the best description of the decay phase of the current (1 exponential χ^2 = 11.6 ± 7.8; two-exponential χ^2 = 0.50 ± 0.15; 23-fold improvement; see *Materials and Methods*). Table 2 summarizes the average exponential components obtained for these fits. As shown in Fig. 2D, receptors desensitized by 98.9 ± 0.3% (n = 6). With increase in the concentration of aniracetam, slower exponential components of desensitization became dominant; initially, a 7-ms component became dominant (Fig. 1B), and at the highest aniracetam concentrations, an additional component of about 30 ms was prominent (Fig. 1C; Table 2). At an intermediate concentration of aniracetam (1 mM), three exponentials were required to fit the entire decay phase, and included the 1-, 7-, and 30-ms components (Fig. 1B, Table 2). At 5 mM, the extent of desensitization, estimated by the extrapolation of the exponential fits to infinite time, was approximately 90.2 ± 1.5% (Fig. 1D).

The deactivation of currents after the rapid removal of glutamate without aniracetam was generally described with a single exponential decay of 500 to 600 μs (Fig. 1D), consistent with previous observations (Raman and Trussell, 1992, 1995b). In the presence of as little as 0.1 mM aniracetam, the time constant of deactivation doubled, doubling yet again at 5 mM (Figs. 1B, 2A, and C). Over the full range of concentrations, deactivation increased from 0.55 ± 0.19 ms (n = 5)

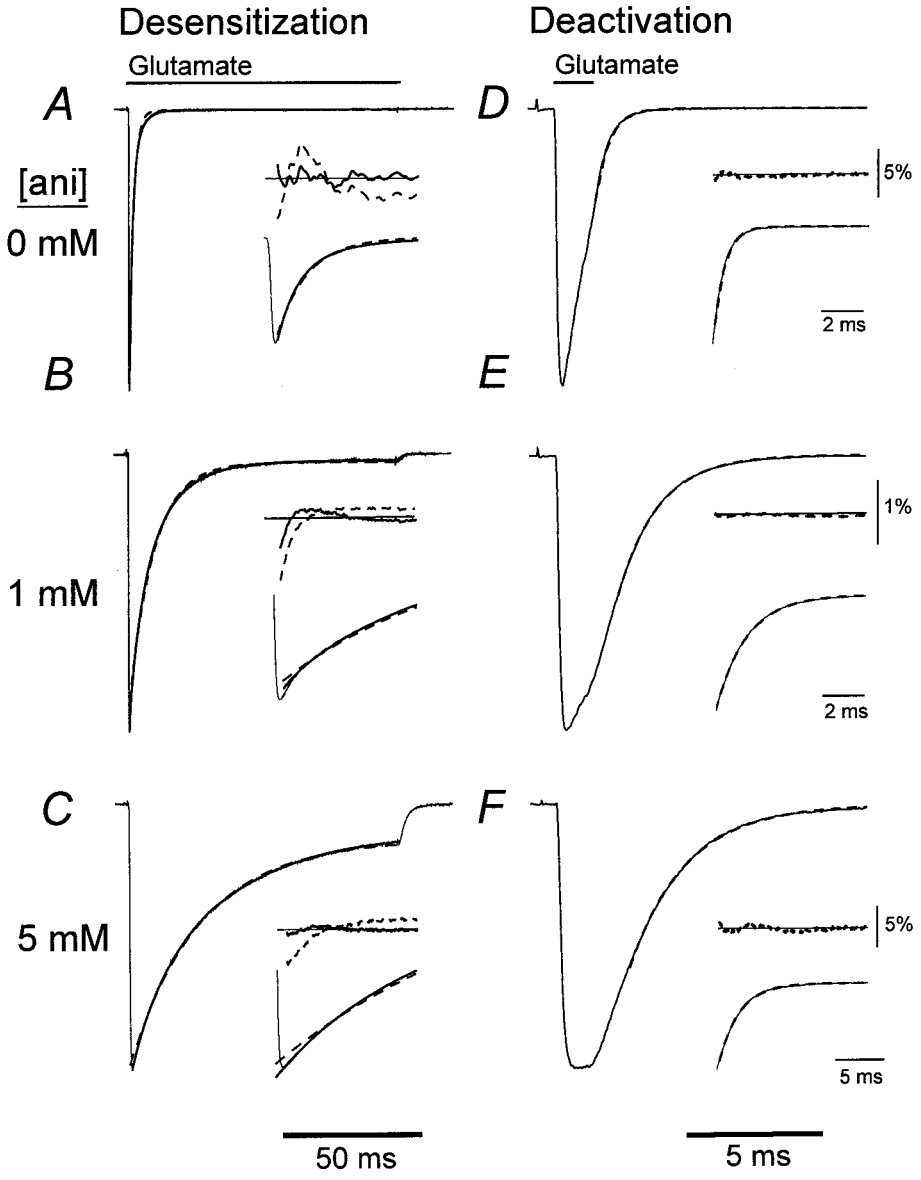

Fig. 1. Dose dependence of desensitization (A–C) and deactivation (D–F) time constants. In each, the traces on the left show a desensitizing response to 10 mM glutamate with the indicated concentration of aniracetam and superimposed exponential fits. Insets, expanded view of fits (bottom inset) and residuals (top inset). A, dashed trace is a single exponential, solid trace is a double exponential with time constants 1 ms (81%) and 3.2 ms. B, dashed line is a single exponential, solid line is a double. A triple exponential is shown but superimposes on the data perfectly; its values are 0.7 ms (20%), 7.6 ms (64%), and 20.1 ms (16%). C, dashed line is a single exponential, solid line is a double exponential with time constants 8.4 ms (23%) and 34 ms. D–E, dashed lines are single exponentials with values of 0.52, 1.55, and 2.16 ms, respectively. Percentage of peak current is indicated on the right of the figure and applies to residuals.

in control to 1.95 ± 0.52 ms (n = 8) with 5 mM aniracetam (Figs. 1F and 2A). Differences in time constant between 1 and 5 mM were not significant (p = 0.24). In simulations (see *Discussion*), it was possible to describe the relationship between deactivation and aniracetam concentration as a steady decrease in α, the rate constant of channel closing (Fig. 2A, dashed line). Although it was not possible to know whether the effects of aniracetam saturated because of drug solubility limits, the majority of its effects on deactivation appeared at 0.1 to 1 mM. We did not consistently observe multiple exponential decays in deactivation.

The magnitude of the effects of aniracetam on desensitization seemed to be larger and occurred at a higher aniracetam concentration than the effects on deactivation. Figure 2B illustrates the results of weighted exponential fits to the onset of desensitization, which provide a convenient index of the overall slowing of the decaying current. The time constant in controls is between 1 and 2 ms (Fig. 2B), doubles in 0.1 mM aniracetam, but is more than 5- and 10-fold longer in 1 and 5 mM aniracetam (Fig. 2C), respectively. Examining the maximal effect of the drug, desensitization slowed from about 1.7 ± 0.1 ms (n = 6) in control to 21.2 ± 1.7 ms (n = 10) in 5 mM aniracetam. Using the same model parameters for Fig. 2A, the slowing of desensitization expected for an action solely on α is shown in Fig. 2B as a dashed line. Clearly, values of α suitable to explain deactivation are not sufficient to account for aniracetam's effects on desensitization. This point is emphasized in Fig. 2C, which plots the dose dependence of the -fold increase in time constants for patches and for the model. Beginning at 1 mM aniracetam, and model parameters suitable to account for deactivation, a sharp deviation from the model predictions were observed for desensitization. Moreover, an effect solely on α was not adequate to account for the increase in steady-state current during long glutamate applications in 3 and 5 mM aniracetam (Fig. 2D). These data indicate that at high concentrations, aniracetam must act on the microscopic rates of entry into desensitized states, in addition to slowing channel closure.

Paired-Pulse Desensitization and Resensitization. When pairs of brief pulses of glutamate are delivered, receptors continue to desensitize between the two applications, despite the absence of free glutamate (Raman and Trussell, 1995b). If a modulator reduced desensitization to brief conditioning pulses, then it must be acting directly on processes unrelated to the rate of opening or closing of the channel, because the channels are closed during the period between the two pulses. Figure 3A, i, illustrates a protocol in which two pulses of 10 mM glutamate were applied to a patch, with the pulses separated by 10 ms and the duration of the first pulse (P1) increased with each repetition of the pair. Responses to P1 reached the same peak even for the briefest applications (compare shortest and longest junction potentials in Fig. 3A, i). For such brief conditioning pulses (~0.45 ms), the second pulse (P2) produced a response 42% smaller than the first (Fig. 3A, ii). As P1 was increased, the response to P2 grew progressively smaller, because of greater desensitization, until a maximum of 62% reduction in the peak at the longest P1 (~3.45 ms; Fig. 3A, iii). Figure 3B, i, illustrates the prediction that paired-pulse desensitization should be resistant to modulators that act only on the channel-closing rate by showing the relative amount amounts of paired-pulse desensitization with brief (Fig. 3B, ii) or long (Fig. 3B, iii) conditioning pulses when the closing rate is changed. Here, the amount of desensitization after a very brief pulse is expected not to change when the closing rate is reduced. Thus, a paired-pulse protocol, measuring the amount of desensitization and its rate of recovery, can be used to determine whether modulators alter particular desensitization steps independent of effects on channel closing rates.

However, in the presence of 3 or 5 mM aniracetam, much less desensitization was apparent even for the briefest initial application (Fig. 3C, i–iii). Figure 3E illustrates data pooled from four patches in which both control (○) and aniracetam (□) was obtained with a wide range of pulse durations. In each patch, the amplitude of P2 was normalized to the amplitude of P1, which corrects for variability among patches and the effects of aniracetam on peak current (see below). The duration of each initial pulse was slightly variable, especially for the briefest pulses, and thus we have plotted the normalized P2 responses against the half-width of the P1 application (see *Materials and Methods*). For short conditioning pulses (mean 0.6 ± 0.1 ms), the average response to P2 was 0.56 ± 0.02 (n = 5) after normalizing to the peak amplitude of the P1 response. For a long conditioning pulse (3.1 ± 0.03 ms), the average was 0.37 ± 0.03. In these same patches, aniracetam increased the amplitude of the response to P1 by 31 ± 13% (3 mM, n = 8) and 37 ± 31% (5 mM, n = 7). For the short pulses (0.6 ± 0.05 ms), the normalized response to P2 was 0.84 ± 0.02 (n = 5), not significantly different from that of the response to long (3.0 ± 0.2 ms) pulses, whose mean normalized amplitude was 0.78 ± 0.02 (p = 0.067, unpaired t test).

These data indicate, first, that desensitization was observed even with the briefest glutamate pulses. Solid exponential curves through the data in Fig. 3E were extrapolated to zero time to estimate the minimal amount of desensitization the receptors would be expected to undergo. These curves intersect the zero time axis at 0.64 for control and 0.86 for aniracetam (Fig. 3D). Thus, in control, a minimum of 36%

TABLE 2

Values and weights for exponential components obtained from fitting the onset of desensitization at 0–5 mM aniracetam

At 0 mM aniracetam (control), the 20% component was omitted for clarity. For 1 mM aniracetam, double exponential fits showed only a 7-fold improvement. All other χ^2 values display the fold-improvement from single- to double-exponential fit.

	χ^2	n	τ_{fast}	$\%_{fast}$	τ_{int}	$\%_{int}$	τ_{slow}	$\%_{slow}$
0	23	6	1.1 ± 0.1	80 ± 9				
0.1 mM	34	6	1.1 ± 0.3	64 ± 11	5.1 ± 0.3	36 ± 11		
0.3 mM	30	5	0.9 ± 0.1	56 ± 10	6.1 ± 1.2	44 ± 10		
1 mM	31[a]	7	0.9 ± 0.4	21 ± 12	7.4 ± 3.3	58 ± 16	25 ± 14	21 ± 12
3 mM	6	3			7.7 ± 2.3	36 ± 29	20 ± 3	64 ± 29
5 mM	20	10			7.0 ± 1.6	33 ± 14	28 ± 5	67 ± 14

[a] The -fold improvement in χ^2 value shown compares a triple exponential to a single exponential fit.

of receptors must desensitize. Even with aniracetam, some desensitization (14%) was obtained with minimal exposure to glutamate.

A second implication of these observations was apparent upon simulations of this experiment using the model discussed below. In Fig. 3E, the solid thick line through the open circles shows the predictions of the kinetic model with the control parameter set. The coincidence of the model and the control data indicate that the model can account for the paired pulse responses reasonably well. When the value of α was changed to account for deactivation in 5 mM aniracetam, the resulting simulation was unable to approximate the experimentally obtained aniracetam data (Fig. 3E, dashed line). Instead, additional modifications were made in two desensitization rates, L_f and M_f, which were reduced 5- and 4.2-fold, respectively. The resulting simulations (Fig. 3E, thick line through open squares) were successful in describing the experimental effects of aniracetam. Thus, these data support the conclusion from Fig. 2 that aniracetam must directly lower the microscopic rates of desensitization.

The paired-pulse desensitization results described above suggested that rates coupled directly to desensitized states may be affected by aniracetam. To determine whether microscopic rates of recovery from desensitization (L_b and/or M_b) are sensitive to aniracetam, we measured recovery after desensitizing pulses of glutamate. In the absence of aniracetam, the recovery rates induced by either a brief or long pulse have been shown to be similar, occurring in an exponential time course of approximately 16 ms (Raman and Trussell, 1995b). In the present study, accumulation into desensitized states was driven by a 20-ms conditioning pulse of glutamate and recovery from desensitization was monitored with 1-ms test pulses at intervals lengthened in 3-ms increments. Example records are shown in Fig. 4A. The amplitude of the test pulse was divided by the amplitude of the first pulse in Fig. 4C. The data were fitted by single exponential of 19 ± 2 ms (n = 3), similar to the value of 16 ms reported previously for these glutamate receptors (Raman and Trussell, 1995b). A short lag in recovery was accounted for by a shift in the time axis of exponential fits, as described previously (Raman and Trussell, 1995b). Recovery from desensitization was then measured in the presence of 5 mM aniracetam using an identical conditioning/test pulse protocol (Fig. 4B), and averaged recovery data are plotted in Fig. 4C. Data were fit with a single exponential of 16 ± 1 ms (n = 8), indicating that the recovery time course of desensitization

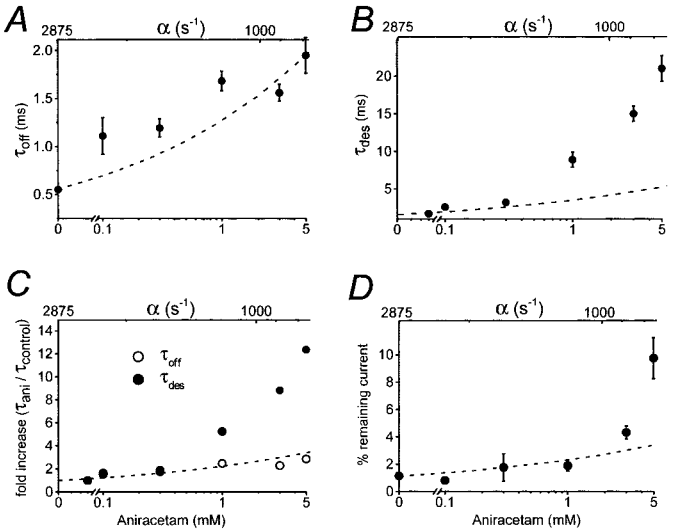

Fig. 2. Aniracetam dose dependence of deactivation (τ_{off}, A), desensitization (τ_{des}, B), the fold increase in these parameters (C), and percentage of remaining current at steady-state (D). Single-exponential fits are used here to simplify comparison. The upper x-axis in each shows ranges of α in the simulations, and the dashed curves are the predicted change in the indicated parameters with graded change in α. The data show that slowing of the channel closing rate accounts well for aniracetam's effects on deactivation, but accounts for the other parameters only at low concentrations.

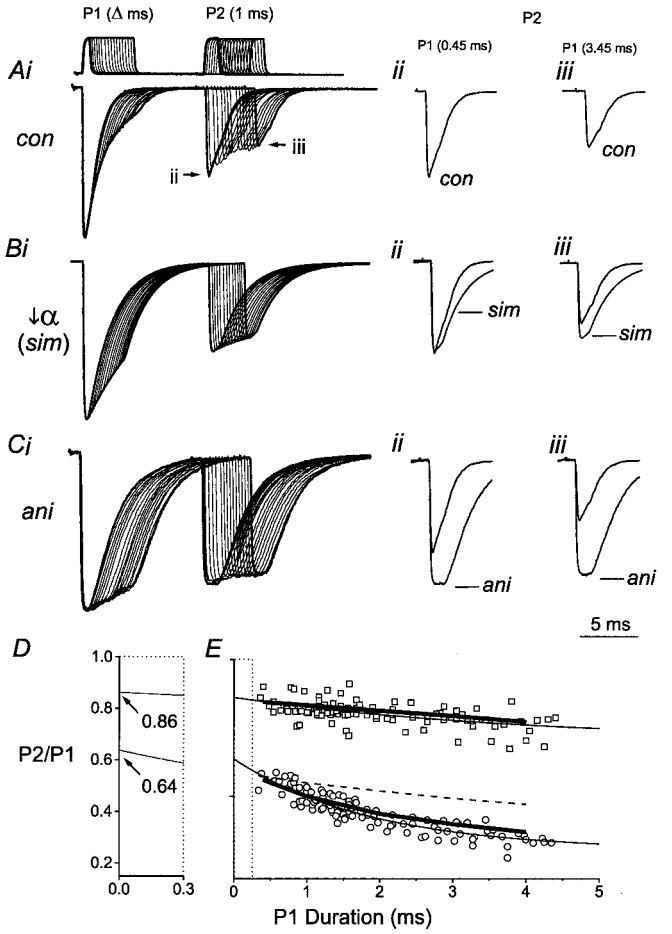

Fig. 3. Paired-pulse desensitization reveals effects of aniracetam directly on entry into desensitized states. Two pulses of 10 mM glutamate 10 ms apart were delivered to a patch in A, i, such that with each trial, the duration of the first pulse (P1) was increased, whereas the second pulse (P2) was 1 ms long. A, ii and iii, show the first and last P2 pulses in isolation. B, i, simulations based on the control parameters with the channel closing rate slowed to account for the slowing of deactivation in 5 mM aniracetam. B, ii and iii, these simulated P2 pulses are compared with the experimental traces from A and show that for the briefest P1 pulse, reducing the closing rate should not alter the relative amplitude of the P2 response. In C, iii, the same patch as in A has been exposed to 5 mM aniracetam, and the paired pulse protocol was repeated. C, ii, shows that in aniracetam, the P2 pulse is much larger; after normalizing for changes in P1, in contrast to the predictions of the model in B. E shows the ratio P2/P1 peak responses versus the duration of P1 in each trial pooled from five patches with control (○) and 3 or 5 mM aniracetam (□) solutions. Solid lines are exponential fits to the data; at their intersection with zero time, shown in D, some desensitization is still predicted. The dashed line is model predictions with only α slowed, as in B; these clearly do not account for the □ data. Thick lines are Table 1 model predictions for control and for aniracetam, with both desensitization and channel closing slowed.

was not markedly altered by aniracetam (unpaired t test, $p = 0.17$). Thus, coupled with evidence that rates directly associated with desensitization must be influenced to account for both the reduction of paired-pulse desensitization and slowing of the rate of desensitization by aniracetam, we suggest that L_f and/or M_f are slowed by aniracetam. Accordingly, simulations using the parameter set described above gave exponential recovery times of 20.3 and 15.6 ms for the control and aniracetam models, respectively.

The measurement of recovery time course gave us the opportunity to test the validity of the model with respect to the observations that recovery proceeds after a delay. This observation (Raman and Trussell, 1995b; Bowie and Lange, 2002; Robert and Howe, 2003) has been taken as evidence of conformational steps preceding the full recovery of desensitized receptors, a feature predicted from recent allosteric models of AMPA receptor gating (Bowie and Lange, 2002; Robert and Howe, 2003). Figure 4D shows that our earlier model (dashed line) also predicts this delay in recovery quite well, deviating markedly from a simple exponential increase in sensitivity (solid black line). This observation indicates that the model is indeed useful for evaluating alterations in receptor function that could account for the action of modulators of desensitization.

Aniracetam Increases Channel Open Probability. Nonstationary variance analysis was employed to estimate the open probability of the AMPA receptor in the presence of 5 mM aniracetam. Patches were exposed at least 30 times to 100-ms pulses of glutamate. The current variance was plotted against the mean current and fitted with a parabola in the form $\delta^2(t) = i \times I(t) - I^2(t)/N$, where $\delta^2(t)$ is the variance, $I^2(t)$ is the mean, i is the single channel current, and N is the number of receptors in the patch (not shown). The peak open probability (P_o) can be calculated from I_{max}/iN, where I_{max} is the maximal current and I and N are from the fit. In three patches from which stable responses were obtained without appreciable run-down of peak current, the P_o was 0.72 ± 0.01, i was 1.9 ± 0.2 [which corresponds to a single-channel conductance (γ) of 26 ± 3 pS], and N was 196 ± 70 channels. These results indicate a higher P_o and γ from that previously observed in the presence of 10 mM glutamate alone, in which P_o was 0.54 ± 0.1 and γ was 18 ± 4 pS (Raman and Trussell, 1995a). For comparison, the model developed here yielded a peak P_o of 0.57 and 0.83 for control and aniracetam.

Aniracetam Does Not Prolong Deactivation in Kainate. The agonist kainate acts on AMPA receptors, generating a current that produces little desensitization but instead rapidly attains a large, steady-state level (Raman and Trussell, 1992). Thus, with kainate, one would expect the AMPA receptor to spend less time in desensitized states (Patneau and Mayer, 1991). However, deactivation of the kainate-induced response, as with glutamate, should still be dependent on the channel-closing rate α. We therefore explored the effect of aniracetam on deactivation in kainate. In contrast to aniracetam's effect on glutamate currents, we found that aniracetam did not significantly affect deactivation of kainate currents (Fig. 5, B and E). Furthermore, neither peak amplitude (Fig. 5C) nor desensitization time constants (Fig. 5, A and E) were affected. However, a small but significant enhancement of steady-state current was detected (Fig. 5D). Thus, the value of α, as well as its sensitivity to aniracetam, seems to depend on the type of agonist. Shen et al. (1999) also observed little effect of aniracetam on current evoked by kainate.

Kinetics of Synaptic Transmission. Excitatory synaptic currents were recorded in nucleus magnocellularis neu-

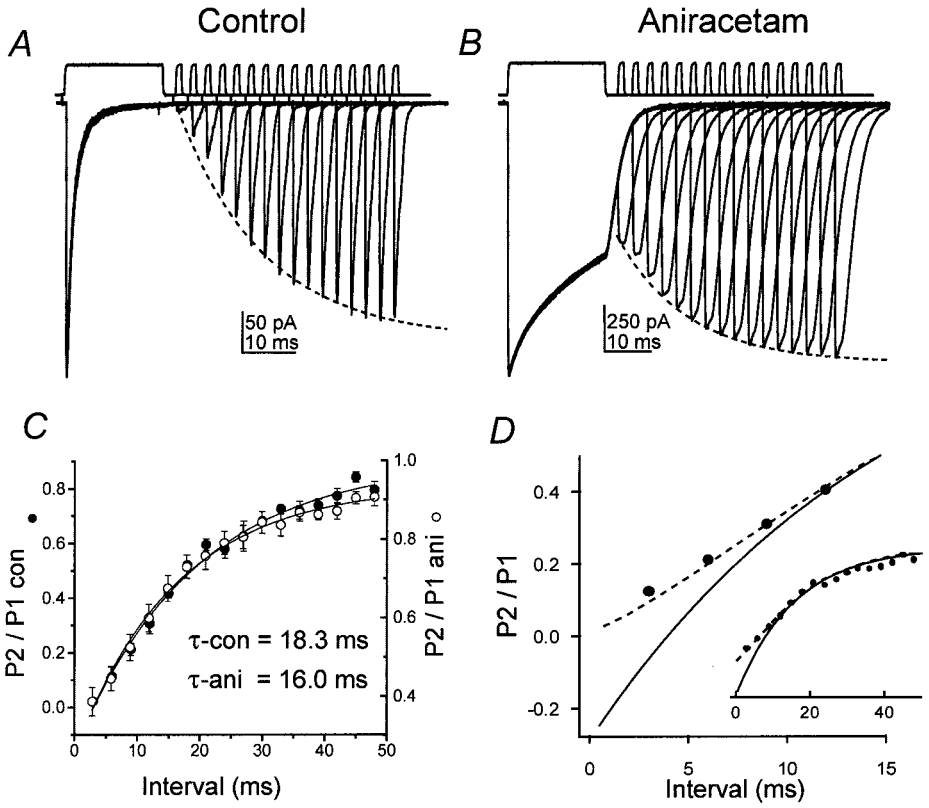

Fig. 4. Recovery from desensitization is not modulated by aniracetam. A, control solutions; B, 5 mM aniracetam. A 20-ms conditioning pulse of agonist (P1) was followed by 1-ms test pulses (P2) at the indicated intervals. The test responses were expressed as P2/P1 at the indicated intervals in C and D. A single exponential curve was fit to the recovery, accounting for a slight delay in the onset of recovery (Raman and Trussell, 1995a), which is evident from the initial deviation of data from the exponentials drawn in A and B. D, control data (black symbols) are superimposed on the predictions of the kinetic model (dashed line) to illustrate that such nonmonotonic recovery is predicted by our kinetic scheme. Solid line is a single exponential curve fit to the major part of the model prediction. Inset, recovery over wider time-base. It was necessary to shift experimental data points upward by 10% to superimpose on the model, but this did not alter their time course.

rons in brain slices to determine how their decay time compares with that of glutamate responses in patches. The sensitivity of these currents to AMPA receptor antagonists, to cyclothiazide, aniracetam, and GYKI 52466 (Trussell et al., 1993; Brenowitz and Trussell, 2001) strongly suggests that they are mediated by the same receptors observed in outside-out patches. In control solutions, channel deactivation and desensitization may be similar in time course to that of transmitter diffusion, complicating comparisons of EPSCs to patch responses. Here, we focused on the responses in the presence of 5 mM aniracetam at room temperature; in this condition, transmitter diffusion after release of single glutamate vesicles should be considerably faster than channel kinetics, so interpretable comparisons between patch and synaptic responses could be made. Figure 6A and Table 3 summarize measurements of kinetics and amplitudes of mEPSCs in control and aniracetam. In addition, we compared the decay time of mEPSCs to deactivating responses in patches, all with aniracetam (Table 3). For cells in which mEPSCs were best fit with a sum of two exponentials, both components increased in aniracetam. The single-exponential decay constants of mEPSCs and deactivating responses in patches were not significantly different. In addition, the increase in amplitude of mEPSCs by aniracetam was similar to the increase observed in patch responses (Table 3). We conclude that receptors in patches and at synapses have similar kinetics and sensitivity to aniracetam. Transmitter clearance times must therefore be considerably faster than 1.5 ms (the decay time constant of mEPSCs in anirecetam). Indeed, because mEPSCs and deactivation is similar even in control solutions (Otis et al., 1996a), clearance of transmitter from one vesicle must be <0.5 ms.

During evoked transmission, EPSC decay times are expected to be broader than mEPSCs, because of temporal dispersion of release and delayed clearance of transmitter. We measured the decay time of evoked EPSCs (eEPSCs) in the presence of 10 μM Cd^{2+} to reduce the quantal content and so reduce the problems of clearance of transmitter from the calyceal synaptic cleft. Experiments were performed by recording eEPSCs first in control solution, then in bath-applied aniracetam, and finally in the presence of aniracetam plus 10 μM Cd^{2+}, applied by pressure application from a nearby pipette. In Fig. 6B, amplitudes and kinetics of eEPSCs are shown for all of these conditions. Aniracetam increased the amplitude of evoked EPSCs to a somewhat larger degree than in mEPSCs and patches (Table 3). Evoked EPSCs rose more slowly after application of aniracetam in low (0.70 ± 0.07 ms) or high (0.83 ± 0.10 ms) release conditions (control 0.45 ± 0.02 ms, $n = 4$). Decay times could be best fit with two exponentials. In aniracetam plus Cd^{2+}, these components were similar to the double exponential decay of mEPSCs in aniracetam (Table 3). For single exponential fits, the decays were also similar (2 and 1.5 ms for eEPSCs and mEPSCs, respectively). These data suggest 1) that aniracetam itself does not cause a severe distortion of the release time course, as has been suggested for cyclothiazide (Diamond and Jahr, 1995), and 2), that the clearance of transmitter is probably faster than the deactivation time of 1.5 to 2 ms.

In solutions in which release was not blocked, eEPSCs decayed much more slowly, as shown in Fig. 6B and Table 3. These values were more than 2-fold longer than the time constants observed in Cd^{2+} or for mEPSCs. Because aniracetam did not markedly prolong the release process itself, the slower decay in high-release conditions is most likely to be an outcome of two factors: slower transmitter diffusion will lead to rebinding and reactivation of receptors, so that the decay would reflect the gradual decline in glutamate levels. However, rebinding will also lead to desensitization, and the kinetics of decay could in part reflect this process. Table 3 summarizes the rates of decay of synaptic events, deactivation in aniracetam, and can be compared with values for desensitization in Table 2. In 5 mM aniracetam, desensitization to step pulses of glutamate occurs with time constants of 7 and 28 ms, the latter being the main component of the fit. eEPSCs in aniracetam decay with a time course that is

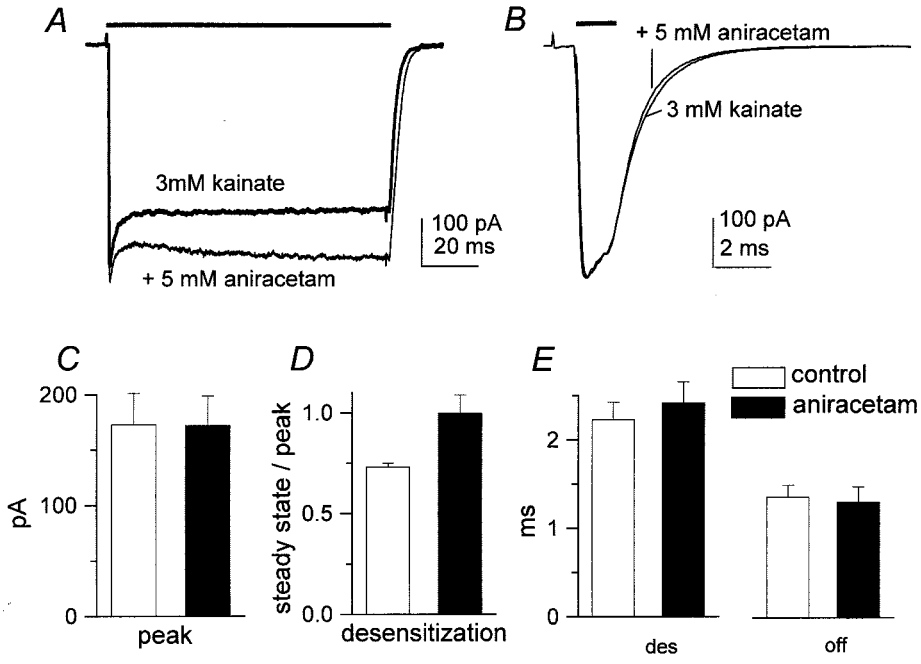

Fig. 5. Aniracetam has little effect on responses to kainate. Aniracetam produces small increase in the steady-state amplitude (A and D) and but has no effect on peak (C) or on time course of desensitization or deactivation (B and E). Traces in A and B from one patch examined in control and aniracetam solutions. C–E, averaged data from 10 patches, except τ_{off} (four patches).

generally faster and suggests that diffusion/rebinding is the dominant factor in shaping the eEPSC under these conditions. More importantly, the data strongly suggests that, under conditions of high release, that glutamate clearance is markedly slower than the time course of desensitization of AMPA receptors in the *absence* of aniracetam (~1 ms; Raman and Trussell, 1995b).

To compare depression of EPSCs to the paired-pulse desensitization described in Fig. 3, we next examined the response to pairs of synaptic stimuli, delivered at 10-ms intervals above. Figure 7, A and B, show that in aniracetam, depression was markedly lessened, as described previously (Brenowitz and Trussell, 2001). Depression arises both from desensitization and from presynaptic effects, such as depletion of transmitter. Assuming no presynaptic effects of aniracetam (Brenowitz and Trussell, 2001), the difference in depression with and without aniracetam should give an estimate of the magnitude of synaptic desensitization. This value, calculated as $PPD_{ani}/PPD_{control}$ for each cell (PPD is defined as the ratio of the second to the first response in the pair), gave an average value of 2.04 ± 0.16 (n = 16) and is plotted in Fig. 7C as a horizontal solid line. For comparison, this same parameter is derived from the exponential fits of data from patches and plotted in Fig. 7C against the interval between pulses (continuous curved line). ■ show the predictions of the model derived above, which agreed well with the data. □ show the predictions for a model in which aniracetam only slows α. With the shortest glutamate pulses, the ratio was about 1.5, increasing to about 2 with the longest pulses. The ratios for synaptic and patch data cross at a P1 of around 4 ms. Thus, the degree of desensitization 10 ms after transmitter release is equivalent to that produced by a square pulse of 10 mM glutamate lasting about 4 ms, with a 10 ms-period of recovery.

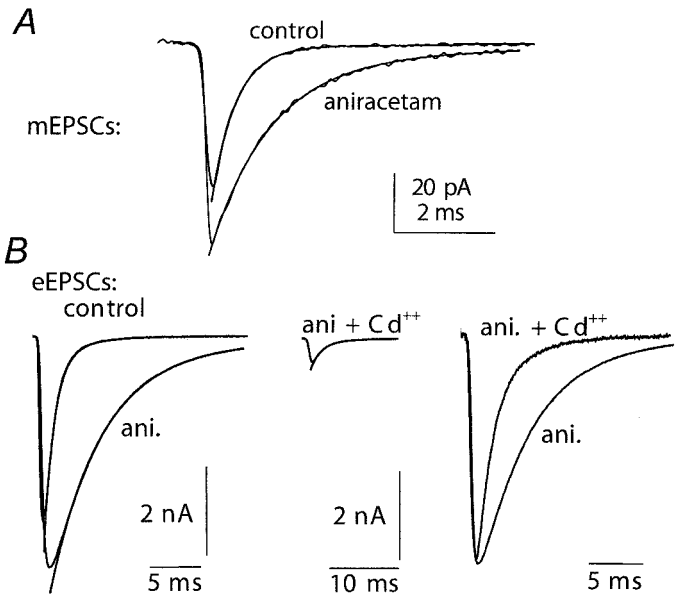

Fig. 6. Effects of aniracetam on EPSC kinetics. A, 5 mM aniracetam slows the decay time of mEPSCs. Averages of 30 to 50 mEPSCs in the same cell. Lines through decay are exponential fits with time constants: control, 0.48 ms; aniracetam, 1.1 ms (90%) and 5 ms. B, evoked EPSCs in control and in aniracetam with and without 10 μM Cd^{2+}. All traces are from one cell. Decay of leftmost and middle traces are fit with exponentials: control, 0.87 (93%) and 3.23 ms; Aniracetam 4.8 (94%) and 18.8 ms; Aniracetam plus Cd^{2+}, 1.43 (87%) and 4.62 ms. In the rightmost traces, the responses in aniracetam with and without Cd^{2+} are scaled to illustrate the large differences in their decay time.

Discussion

Effects of Aniracetam on Receptors in Patches. Aniracetam increased the amplitude and decay time of responses to glutamate by two mechanisms. At lower concentrations, the drug slowed channel gating, as proposed in previous studies (Partin et al., 1996; Suppiramaniam et al., 2001). Consequently, both the rates of deactivation and desensitization were slowed. Indeed, the slowing of desensitization is clearly linked to the slowing of deactivation at concentrations of aniracetam <1 mM. Stabilization of the open conformation would also be expected to increase the peak amplitude of responses, before the onset of desensitization. However, at higher concentrations of aniracetam, we observed a further slowing and lessening of desensitization, beyond what would be predicted from an effect solely on channel gating but without further slowing of deactivation. Such an action suggested that binding of additional aniracetam molecules had an effect directly upon the rates governing entry into desensitized states. This conclusion was further supported by two observations. First, paired-pulse desensitization was markedly reduced by aniracetam, an effect not expected from a slowing of channel closure. Second, the rate of recovery from desensitization was only slightly faster in aniracetam. All of these effects could be explained in our model by a dual action of the drug. The fact that effects on deactivation and additional slowing of desensitization had different dose dependence suggests that desensitization can be controlled independently of deactivation. Such a conclusion is consistent with the fact that different AMPA receptor subunits exhibit similar deactivation rates but very different desensitization rates (Mosbacher et al., 1994; Koike et al., 2000). Thus, in native receptors, desensitization is a process fundamentally different from channel closure.

Based on these differences in the dose dependence of deactivation and desensitization, it seems likely that aniracetam can have a significant effect with only a fraction of the subunits occupied by the drug. Current models of AMPA receptor gating suggest that receptors may open to subconductance states when a fraction of the subunits is bound to glutamate (Rosenmund et al., 1998; Smith and Howe, 2000).

TABLE 3

Glutamate-evoked and synaptic currents in the presence of 5 mM aniracetam

Values are presented as means ± S.E.M. N values are the same for each row, unless otherwise noted. Desensitization values found in Table 2.

	Peak Increase	τ_{single}	τ_{fast}	$\%_{fast}$	τ_{slow}
Deactivation	37 ± 31%(n=7)	1.95 ± 0.52(n=8)			
mEPSCs	44 ± 6% (n=5)	1.53 ± 0.08(n=5)	1.17 ± 0.07	89.5 ± 1.66	5.84 ± 1.40
eEPSC-Cd^{2+}		2.07 ± 0.14(n=4)	1.56 ± 0.09	92.18 ± 2.06	8.06 ± 1.98
eEPSC-Ca^{2+}	52 ± 9% (n=6)	4.50 ± 0.61(n=6)	3.72 ± 0.62	93.3 ± 2.6	20.65 ± 4.60

It might be expected then that aniracetam slows the gating for a fraction of the subunits, and this should result in multiphasic decay, with slower components increasing in amplitude with increase in aniracetam concentration. Unfortunately, biphasic deactivation was difficult to resolve in each case. The apparently low affinity of aniracetam also complicates the analysis, because the drug may unbind and rebind during the course of deactivation.

At higher concentrations of aniracetam, the magnitude of the effects on deactivation and desensitization diverged sharply, implying that desensitization is controlled by coordinate properties of multiple subunits. This theme has been explored by several recent studies examining the biophysical properties of recombinant AMPA receptors. Robert et al. (2001), expressed mixtures of desensitizing and largely nondesensitizing (mutant) subunits and found that different rates of desensitization were dependent on the stoichiometry of the mixture. With receptors composed of equal parts of the two subunit types, receptors desensitized with fast, intermediate, and very slow decay times. Their interpretation was that the intermediate component arose from receptors that contained some mutant subunits that conferred both slower deactivation and desensitization to the receptor. In their view, only when the receptor contained at least two mutant subunits present as dimers did the receptor lose most of its desensitization; thus, a critical subunit structure determined desensitization of the whole receptor. In the present study, increase in aniracetam concentration produced distinct shifts in the rate of desensitization reminiscent of the results of Robert et al. (2001) At low aniracetam concentrations, the desensitization onset (~7 ms τ) was similar to that predicted by the observed slowing of channel closure. At higher concentrations, a still slower rate of 20 to 30 ms emerged that eventually dominated the decay process. Presumably, when a critical number of aniracetam molecules bind the receptor, a global shift in desensitization is effected that is distinct from the processes governing the rate of channel closure.

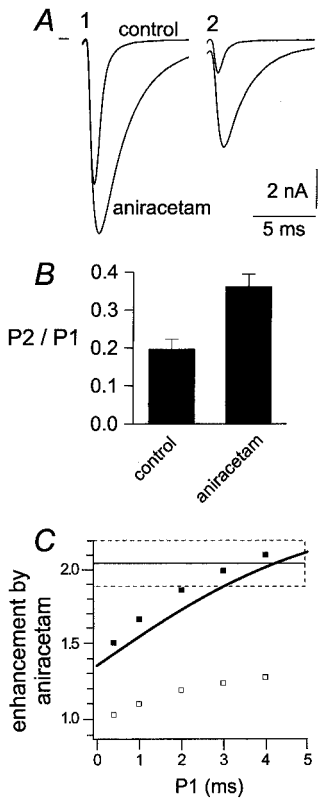

Fig. 7. Paired-pulse depression (PPD) is modulated by aniracetam. A, two EPSCs evoked at a 10-ms interval in control and 5 mM aniracetam solutions. Both EPSCs are increased by aniracetam, but the second of the pair is affected more. B, the ratio of the second to the first response as a measure of the degree of depression (n = 16). C, the solid curve shows the ratio of the exponential curves from Fig. 3E (P2/P1 for aniracetam and control) as a function of the duration of the P1 pulse in that figure. The analogous measurement in synaptic recordings is the ratio of PPD values (calculated as in B) in aniracetam and control, and its mean value is shown as a horizontal line, with ± 1 S.D. as dashed lines. As the duration of P1 increased, desensitization in control and aniracetam solutions diverged. At a P1 of about 4 ms, the difference was equal to the difference in depression for control and aniracetam in EPSC depression. ■ and □ show predictions of the model with parameters as in Table 1 or only with α reduced, respectively.

Sun et al. (2002) examined the properties of recombinant receptors with mutations affecting desensitization or with the modulator cyclothiazide, contrasting these with the changes in affinity between pairs of subunit fragments. They concluded that desensitization is associated with, or caused by, a destabilization of subunit dimers, and that cyclothiazide acts by binding between subunits and disturbing the change in dimer affinity. It is not yet clear where aniracetam binds in the AMPA receptor, and binding between subunits is a possibility. One issue not addressed in that study, however, was how pairs of dimers, which form the receptor, interact during the process of desensitization. Together with the interpretations of Robert et al. (2001), it may be that failure of a single dimer to undergo the structural arrangements characteristic of desensitization will prevent the entire receptor from desensitizing. If, in our experiments, the full effect of aniracetam was associated with binding at both dimer pairs, then it may be that interactions *between* dimer pairs are part of the process of desensitization as well. However, aniracetam is a very low-affinity agent, and it remains possible that the effects we observe reflects multiple binding events within single dimers. This possibility is compounded by the possible heteromeric structure of auditory AMPA receptors, containing glutamate receptors 3 and 4 flop, which could present binding sites of different affinity (Wang et al., 1998; Ravindranathan et al., 2000; Gardner et al., 2001).

Aniracetam As a Tool to Probe Synaptic Transmission. Previous studies suggested that, in nucleus magnocellularis, transmitter could desensitize receptors, but it was not clear whether synaptic desensitization occurred by transmitter rebinding or if it was instead a reflection of that fraction of receptors that desensitize immediately after binding glutamate (Otis et al., 1996b). In this study, this issue was approached first by detailed comparison of EPSCs to the responses to glutamate in patches, all in the presence of aniracetam. We found that the deactivation rate was similar to the decay time of mEPSCs or of evoked EPSCs under conditions of low quantal content. However, these decay times were markedly slower than that of evoked EPSCs of high quantal content (i.e., without Cd^{2+}). In the absence of aniracetam, desensitization is quite rapid (τ of ~1 ms) and so it is difficult to infer the relative contributions to the EPSC decay of desensitization, transmitter diffusion, and transmitter release time course. In the presence of the drug, however, the EPSC decay was slower than the release time course and intermediate between deactivation and desensitization.

Thus, these data indicate that transmitter clearance during the unblocked, evoked EPSC is slow, lasting at least several ms, and therefore must lead to rebinding and reactivation of receptors. Given the speed of desensitization in control solutions (Raman and Trussell, 1995b), the data support the idea that some desensitization may occur by rebinding of transmitter.

Experiments with paired synaptic stimuli support this conclusion. The extent of protection from depression by aniracetam was similar to that seen for a glutamate stimulus delivered 10 ms after a 4-ms square pulse of 10 mM glutamate. Although the actual concentration transient is certainly smaller and slower than this (Otis et al., 1996a; Sakaba and Neher, 2001), it should be noted that if clearance were significantly faster, the effect of aniracetam on depression would have been less: based on the data on patches, with the briefest exposure to glutamate, aniracetam should have increased the size of the scaled second EPSC by only 40%. Instead, the EPSC was doubled, suggesting that the glutamate transient lasts long enough to cause significant rebinding and additional desensitization.

Acknowledgments

We thank Indira Raman, Caitlin Smith, and Tao Lu for comments.

References

Arai A, Kessler M, Ambros-Ingerson J, Quan A, Yigiter E, Rogers G, and Lynch G (1996) Effects of a centrally active benzoylpyrrolidine drug on AMPA receptor kinetics. *Neuroscience* **75:**573–585.

Arai AC, Kessler M, Rogers G, and Lynch G (2000) Effects of the potent ampakine CX614 on hippocampal and recombinant AMPA receptors: interactions with cyclothiazide and GYKI 52466. *Mol Pharmacol* **58:**802–813.

Bowie D and Lange GD (2002) Functional stoichiometry of glutamate receptor desensitization. *J Neurosci* **22:**3392–3403.

Brenowitz S and Trussell LO (2001) Minimizing synaptic depression by control of release probability. *J Neurosci* **21:**1857–1867.

Diamond JS and Jahr CE (1995) Asynchronous release of synaptic vesicles determines the time course of the AMPA receptor-mediated EPSC. *Neuron* **15:**1097–1107.

Gardner SM, Trussell LO, and Oertel D (2001) Correlation of AMPA receptor subunit composition with synaptic input in the mammalian cochlear nuclei. *J Neurosci* **21:**7428–7437.

Hausser M and Roth A (1997) Dendritic and somatic glutamate receptor channels in rat cerebellar Purkinje cells. *J Physiol* **501:**77–95.

Heckmann M and Dudel J (1997) Desensitization and resensitization kinetics of glutamate receptor channels from *Drosophila* larval muscle. *Biophys J* **72:**2160–2169.

Isaacson JS and Nicoll RA (1991) Aniracetam reduces glutamate receptor desensitization and slows the decay of fast excitatory synaptic currents in the hippocampus. *Proc Natl Acad Sci USA* **88:**10936–10940.

Koike M, Tsukada S, Tsuzuki K, Kijima H, and Ozawa S (2000) Regulation of kinetic properties of GluR2 AMPA receptor channels by alternative splicing. *J Neurosci* **20:**2166–2174.

Lawrence JJ and Trussell LO (2000) Long-term specification of AMPA receptor properties after synapse formation. *J Neurosci* **20:**4864–4870.

Mosbacher J, Schoepfer R, Monyer H, Burnashev N, Seeburg PH, and Ruppersberg JP (1994) A molecular determinant for submillisecond desensitization in glutamate receptors. *Science (Wash DC)* **266:**1059–1062.

Otis TS, Wu YC, and Trussell LO (1996a) Delayed clearance of transmitter and the role of glutamate transporters at synapses with multiple release sites. *J Neurosci* **16:**1634–1644.

Otis T, Zhang S, and Trussell LO (1996b) Direct measurement of AMPA receptor desensitization induced by glutamatergic synaptic transmission. *J Neurosci* **16:**7496–7504.

Parks TN (1981) Morphology of axosomatic endings in an avian cochlear nucleus: nucleus magnocellularis of the chicken. *J Comp Neurol* **203:**425–440.

Partin KM, Fleck MW, and Mayer ML (1996) AMPA receptor flip/flop mutants affecting deactivation, desensitization, and modulation by cyclothiazide, aniracetam and thiocyanate. *J Neurosci* **16:**6634–6647.

Patneau DK and Mayer ML (1991) Kinetic analysis of interactions between kainate and AMPA: evidence for activation of a single receptor in mouse hippocampal neurons. *Neuron* **6:**785–798.

Raman IM and Trussell LO (1992) The kinetics of the response to glutamate and kainate in neurons of the avian cochlear nucleus. *Neuron* **9:**173–186.

Raman IM and Trussell LO (1995a) Concentration-jump analysis of voltage-dependent conductances activated by glutamate and kainate in neurons of the avian cochlear nucleus. *Biophys J* **69:**1868–1879.

Raman IM and Trussell LO (1995b) The mechanism of alpha-amino-3-hydroxy-5-methyl-4-isoxazolepropionate receptor desensitization after removal of glutamate. *Biophys J* **68:**137–146.

Raman IM, Zhang S, and Trussell LO (1994) Pathway-specific variants of AMPA receptors and their contribution to neuronal signaling. *J Neurosci* **14:**4998–5010.

Ravindranathan A, Donevan SD, Sugden SG, Greig A, Rao M, and Parks TN (2000) Contrasting molecular composition and channel properties of AMPA receptors on chick auditory and brainstem motor neurons. *J Physiol* **523:**667–684.

Robert A and Howe JR (2003) How AMPA receptor desensitization depends on receptor occupancy. *J Neurosci* **23:**847–858.

Robert A, Irizarry SN, Hughes TE, and Howe JR (2001) Subunit interactions and AMPA receptor desensitization. *J Neurosci* **21:**5574–5586.

Rosenmund C, Stern-Bach Y, and Stevens CF (1998) The tetrameric structure of a glutamate receptor channel. *Science (Wash DC)* **280:**1596–1599.

Sakaba T and Neher E (2001) Quantitative relationship between transmitter release and calcium current at the calyx of held synapse. *J Neurosci* **21:**462–476.

Shen Y, Lu T, and Yang XL (1999) Modulation of desensitization at glutamate receptors in isolated crucian carp horizontal cells by concanavalin A, cyclothiazide, aniracetam and PEPA. *Neuroscience* **89:**979–990.

Smith TC and Howe JR (2000) Concentration-dependent substate behavior of native AMPA receptors. *Nat Neurosci* **3:**992–997.

Sun Y, Olson R, Horning M, Armstrong N, Mayer M, and Gouaux E (2002) Mechanism of glutamate receptor desensitization. *Nature (Lond)* **417:**245–253.

Suppiramaniam V, Bahr BA, Sinnarajah S, Owens K, Rogers G, Yilma S, and Vodyanoy V (2001) Member of the Ampakine class of memory enhancers prolongs the single channel open time of reconstituted AMPA receptors. *Synapse* **40:**154–158.

Tang CM, Shi QY, Katchman A, and Lynch G (1991) Modulation of the time course of fast EPSCs and glutamate channel kinetics by aniracetam. *Science (Wash DC)* **254:**288–290.

Trussell LO, Zhang S, and Raman IM (1993) Desensitization of AMPA receptors upon multi-quantal neurotransmitter release. *Neuron* **10:**1185–1196.

Vyklicky L Jr, Patneau DK, and Mayer ML (1991) Modulation of excitatory synaptic transmission by drugs that reduce desensitization at AMPA/kainate receptors. *Neuron* **7:**971–984.

Wang YX, Wenthold RJ, Ottersen OP, and Petralia RS (1998) Endbulb synapses in the anteroventral cochlear nucleus express a specific subset of AMPA-type glutamate receptor subunits. *J Neurosci* **18:**1148–1160.

Address correspondence to: Dr. Laurence Trussell, Auditory Neuroscience, L-335A, Oregon Health Sciences University, 3181 SW Sam Jackson Park Rd., Portland OR 97239. E-mail: trussell@ohsu.edu